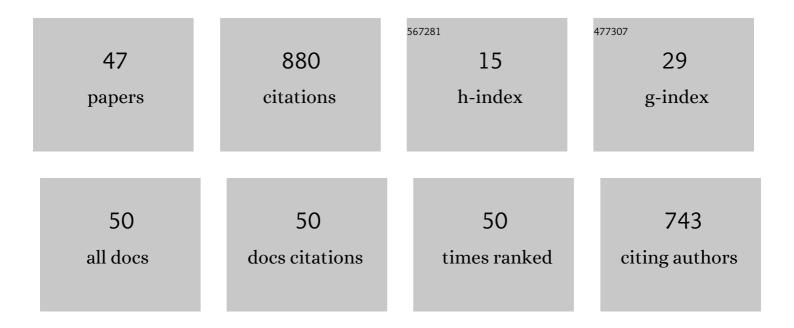
## Igor M Savukov

List of Publications by Year in descending order

Source: https://exaly.com/author-pdf/9187558/publications.pdf Version: 2024-02-01



#	Article	IF	CITATIONS
1	Gradient Field Detection Using Interference of Stimulated Microwave Optical Sidebands. Physical Review Letters, 2022, 128, 163602.	7.8	2
2	Dynamic Nuclear Polarization Enhanced Nuclear Spin Optical Rotation. Angewandte Chemie - International Edition, 2021, 60, 8823-8826.	13.8	5
3	Dynamic Nuclear Polarization Enhanced Nuclear Spin Optical Rotation. Angewandte Chemie, 2021, 133, 8905-8908.	2.0	1
4	Broadband Ultra-Sensitive Adiabatic Magnetometer. , 2021, , .		1
5	Relativistic Configuration-Interaction and Perturbation Theory Calculations for Heavy Atoms. Atoms, 2021, 9, 104.	1.6	3
6	Relativistic Configuration-Interaction and Perturbation Theory Calculations of the Sn XV Emission Spectrum. Atoms, 2021, 9, 96.	1.6	1
7	Detection of ultra-low field NMR signal with a commercial QuSpin single-beam atomic magnetometer. Journal of Magnetic Resonance, 2020, 317, 106780.	2.1	15
8	Parallel high-frequency magnetic sensing with an array of flux transformers and multi-channel optically pumped magnetometer for hand MRI application. Journal of Applied Physics, 2020, 128, .	2.5	3
9	Configuration–Interaction Perturbation Theory Calculations of Pu II. Atoms, 2020, 8, 39.	1.6	1
10	CI-MBPT and Intensity-Based Lifetime Calculations for Th II. Atoms, 2020, 8, 87.	1.6	1
11	Relativistic configuration-interaction and many-body-perturbation-theory calculations of U i hyperfine constants. Physical Review A, 2020, 102, .	2.5	4
12	CI-MBPT line strengths and atomic probabilities for some transitions of neutral iodine. Journal of Physics B: Atomic, Molecular and Optical Physics, 2020, 53, 145003.	1.5	4
13	Investigation of magnetic noise from conductive shields in the 10–300 kHz frequency range. Journal of Applied Physics, 2020, 128, 234501.	2.5	4
14	Accurate CI-MBPT calculation of radiative lifetimes and transition probabilities of neutral lanthanum (La I) odd states with J = 3/2. Physica Scripta, 2020, 95, 105401.	2.5	3
15	Diamond magnetometer enhanced by ferrite flux concentrators. Physical Review Research, 2020, 2, .	3.6	78
16	Calculations of neon nuclear-spin optical rotation, Verdet and hyperfine constants with configuration-interaction many-body perturbation theory. European Physical Journal D, 2019, 73, 1.	1.3	1
17	Experimental limit on an exotic parity-odd spin- and velocity-dependent interaction using an optically polarized vapor. Nature Communications, 2019, 10, 2245.	12.8	20
18	Magnetocardiography with a 16-channel fiber-coupled single-cell Rb optically pumped magnetometer. Applied Physics Letters, 2019, 114, .	3.3	64

IGOR M SAVUKOV

#	Article	IF	CITATIONS
19	Configuration-interaction many-body perturbation theory for La ii electric-dipole transition probabilities. Physical Review A, 2019, 99, .	2.5	5
20	Highly sensitive multi-channel atomic magnetometer. , 2018, , .		2
21	CI+MBPT calculations of Ar I energies, <i>g</i> factors, and transition line strengths. Journal of Physics B: Atomic, Molecular and Optical Physics, 2018, 51, 065006.	1.5	2
22	Experimental Constraint on an Exotic Spin- and Velocity-Dependent Interaction in the Sub-meV Range of Axion Mass with a Spin-Exchange Relaxation-Free Magnetometer. Physical Review Letters, 2018, 121, 091802.	7.8	29
23	Multinuclear Detection of Nuclear Spin Optical Rotation at Low Field. Journal of Physical Chemistry Letters, 2018, 9, 3323-3327.	4.6	8
24	Magnetic microscopic imaging with an optically pumped magnetometer and flux guides. Applied Physics Letters, 2017, 110, .	3.3	10
25	High-resolution magnetic imaging with an array of flux guides. , 2017, , .		1
26	Parametric CI+MBPT calculations of Th I energies andg-factors for even states. Journal of Physics B: Atomic, Molecular and Optical Physics, 2017, 50, 165001.	1.5	8
27	A High-Sensitivity Tunable Two-Beam Fiber-Coupled High-Density Magnetometer with Laser Heating. Sensors, 2016, 16, 1691.	3.8	11
28	Spin-exchange relaxation-free magnetometer with nearly parallel pump and probe beams. Measurement Science and Technology, 2016, 27, 055002.	2.6	38
29	Ultra-sensitive Magnetic Microscopy with an Optically Pumped Magnetometer. Scientific Reports, 2016, 6, 24773.	3.3	36
30	Milli-tesla NMR and spectrophotometry of liquids hyperpolarized by dissolution dynamic nuclear polarization. Journal of Magnetic Resonance, 2016, 270, 71-76.	2.1	14
31	Gradient-echo 3D imaging of Rb polarization in fiber-coupled atomic magnetometer. Journal of Magnetic Resonance, 2015, 256, 9-13.	2.1	8
32	CHAPTER 7. Detection Using SQUIDs and Atomic Magnetometers. New Developments in NMR, 2015, , 183-224.	0.1	0
33	Multi-flux-transformer MRI detection with an atomic magnetometer. Journal of Magnetic Resonance, 2014, 249, 49-52.	2.1	12
34	Non-cryogenic ultra-low field MRI of wrist–forearm area. Journal of Magnetic Resonance, 2013, 233, 103-106.	2.1	9
35	Anatomical MRI with an atomic magnetometer. Journal of Magnetic Resonance, 2013, 231, 39-45.	2.1	34
36	SQUIDs vs. Induction Coils for Ultra-Low Field Nuclear Magnetic Resonance: Experimental and Simulation Comparison. IEEE Transactions on Applied Superconductivity, 2011, 21, 465-468.	1.7	25

IGOR M SAVUKOV

#	Article	IF	CITATIONS
37	Noise Modeling From Conductive Shields Using Kirchhoff Equations. IEEE Transactions on Applied Superconductivity, 2011, 21, 489-492.	1.7	8
38	Non-cryogenic anatomical imaging in ultra-low field regime: Hand MRI demonstration. Journal of Magnetic Resonance, 2011, 211, 101-108.	2.1	22
39	Progress on Detection of Liquid Explosives Using Ultra-Low Field MRI. IEEE Transactions on Applied Superconductivity, 2011, 21, 530-533.	1.7	16
40	Microtesla MRI with dynamic nuclear polarization. Journal of Magnetic Resonance, 2010, 207, 78-88.	2.1	39
41	Diverse, successful, and fascinating relativistic many-body perturbation theory. Canadian Journal of Physics, 2009, 87, 35-39.	1.1	0
42	Applications of Ultra-Low Field Magnetic Resonance for Imaging and Materials Studies. IEEE Transactions on Applied Superconductivity, 2009, 19, 835-838.	1.7	23
43	SQUID-Based Microtesla MRI for In Vivo Relaxometry of the Human Brain. IEEE Transactions on Applied Superconductivity, 2009, 19, 823-826.	1.7	50
44	MRI with an atomic magnetometer suitable for practical imaging applications. Journal of Magnetic Resonance, 2009, 199, 188-191.	2.1	89
45	Detection of 3He spins with ultra-low field nuclear magnetic resonance employing SQUIDs for application to a neutron electric dipole moment experiment. Journal of Magnetic Resonance, 2008, 195, 129-133.	2.1	5
46	Microtesla MRI of the human brain combined with MEG. Journal of Magnetic Resonance, 2008, 194, 115-120.	2.1	159
47	Wave-plate retarders based on overhead transparencies. Applied Optics, 2007, 46, 5129.	2.1	5